Solid Freeform Fabrication 2023: Proceedings of the 34th Annual International Solid Freeform Fabrication Symposium – An Additive Manufacturing Conference
Reviewed Paper

Effect of surface state and material on surface quality enhancement by Dual Laser Powder Bed Fusion

D. Ordnung*, J. Metelkova, and B. Van Hooreweder

* Department of Mechanical Engineering, KU Leuven, 3001 Leuven, Belgium

Abstract

Parts produced by Laser Powder Bed Fusion typically exhibit a limited surface quality often requiring systematic post-processing. The KU Leuven AM team recently developed a Dual Laser Powder Bed Fusion strategy to improve the quality of inclined up-facing surfaces during building. It consists of two steps: (1) a pulsed laser induces shock waves to remove powder from inclined surfaces, followed by (2) in-situ laser remelting of the newly exposed surfaces. The first part of this paper covers the powder removal efficiency using shock waves depending on the used material. A design of experiments was performed for horizontal samples of tool steels, titanium and aluminium alloys. The second part deals with the effect of the initial surface state on the powder removal efficiency for inclined surfaces ($Sa_{R,LT60}$=16.2 µm, $Sa_{R,LT120}$=24.0 µm). Finally, the third part demonstrates the surface quality improvement, resulting in a reduction of Ra up to 61% for 15° inclinations.

Introduction

Metal parts produced by Laser Powder Bed Fusion (LPBF) typically exhibit a poor surface quality compared to conventionally manufactured parts. In particular, inclined up-facing surfaces pose a significant challenge as they are affected by so-called staircase and edge effects [1, 2]. Therefore, these surfaces usually require additional post-processing (e.g. machining) since they are inaccessible for surface treatment during LPBF. To address this issue, a Dual Laser Powder Bed Fusion (DLPBF) technique has been recently introduced to directly improve the quality of inclined up-facing surfaces during LPBF [3]. It is achieved with a modified commercial single-scanner LPBF setup enabling a consecutive operation of a continuous wave IR laser and a nanosecond pulsed IR laser, both working at 1060 nm wavelength. The technique consists of two steps: (1) using the pulsed laser to locally and selectively create shock waves which remove powder that is covering inclined surfaces, followed by (2) in-situ laser remelting of the newly exposed surfaces.

Powder removal via shock waves is based on laser ablation, a technique that uses high intensity laser pulses to vaporize material. Laser pulses interact with the solid metal surface, which rapidly heats up and vaporizes if the vaporization temperature is exceeded. The generated metal vapor plume is ionized upon interacting with subsequent laser pulses, creating a plasma plume [4]. The rapid expansion of the plasma plume induces radially propagating pressure waves known as laser-induced shock waves. The onset and strength of these shock waves is highly dependent on the specific material properties of the target such as absorptivity, density, thermal conductivity, melting and vaporization thresholds. The phenomenon of laser-induced shock waves is described in detail in [5, 6].

Laser-induced shock waves are typically an undesired process by-product in LPBF, as they can blow away powder particles and molten metal preventing the formation of a stable track [7]. The authors of this paper exploited this phenomenon to remove powder from inclined surfaces, enabling subsequent improvement of the newly exposed surface via in-situ laser remelting. Previous studies on maraging steel M300 investigated various process parameters such as pulse energy, pulse-to-pulse distance, pulse duration and scan strategy, on the efficiency of powder removal [3, 8].

Although the previous studies [3, 8, 9] have demonstrated a significant quality improvement of inclined up-facing surfaces, the efficiency of this technique applied to other AM materials remains unexplored, as does the effect of the initial surface roughness. This study showcases the feasibility of the DLPBF technique for treating various AM materials (M300, M789, A205, Ti64), based on a design of experiments including several pulsed laser parameters (pulse-to-pulse distance, pulse duration, pulse energy). Then, the efficiency of powder removal from 15° inclined surfaces is assessed, considering M789 parts with variable initial surface state (built with a standard and increased layer thickness). Finally, in-situ quality improvement of the aforementioned M789 parts with inclined surfaces is demonstrated by combining selective powder removal and laser remelting during LPBF.

Methodology

Powder removal process study on horizontal surfaces

To evaluate the disturbance of the powder bed generated by shock waves, Fig. 1a shows a centered sample of 6 x 6 x 4 mm built by LPBF from different materials (M300, M789, A205, Ti64). For details on those four widely used materials used in AM and for the corresponding LPBF process parameter optimization the reader is referred to [10, 11, 12, 13] respectively. After building the last layer, the horizontal surfaces of the parts were scanned with variable pulsed laser parameters (Table 1) based on a Taguchi L9 design of experiments [8], inducing a disturbance of the surrounding powder bed. The samples were surrounded by a frame of 26 x 26 x 4 mm (Fig. 1a). In order to quantify the powder bed disturbance, the area inside the frame was scanned with the continuous wave (CW) laser (see fixation parameters in Table 2), gently melting the loose powder and hence fixing its shape. The disturbed powder bed was examined over an area of 1.3 x 25.4 mm (Fig. 1d) using a confocal focus variation microscope Sensofar S-Neox. The measured 3D data were filtered using a Gaussian filter, removing wavelengths < 250 µm. Following the analysis method described in detail in [8], the inner length of the disturbed powder bed was defined based on the calculated mean profile. The results show the mean inner disturbance length L_i based on $L_i(1)$ and $L_i(2)$.

Powder removal applied to inclined surfaces

The powder removal efficiency on inclined surfaces was assessed on 15° inclined M789 parts of variable initial surface state, resulting from using a standard or extremely high layer thickness of 60 µm and 120 µm (LT60 and LT120), respectively. As illustrated in Fig. 1b, after building the last layer, the pulsed laser was used to remove the powder from the inclined surfaces, while varying the number of scan passes (Table 1). After the powder removal step, the inclined surface area was scanned with the CW laser in order to fix the partially removed powder (Table 2). The amount of removed powder was quantified by the mean cleaned length L_c based on the measured maximum and minimum cleaned length $L_c(max)$ and $L_c(min)$, respectively, as defined in Fig. 1b. L_c was then compared to the full part length L_{ref}. Images of the cleaned surfaces were captured with a 3D digital microscope Keyence VHX-6000.

Surface quality improvement by powder removal and subsequent laser remelting

Quality improvement was demonstrated on M789 parts with 15° inclined surfaces for LT60 and LT120 parts (Fig. 1c). Similarly to the previous experiment on inclined surfaces, after building the entire sample, the powder was removed from the inclined surface using pulsed laser and remelted using CW laser in order to improve the surface quality. Powder removal was done by scanning along the surface slope with the pulsed laser, starting from the accessible horizontal top surface towards the covered end of the inclination. The parameters are based on findings from [3, 8] and given in Table 1, except for the number of scan passes $N = 15$ and $N = 20$ for LT60 and LT120, respectively. Subsequent laser remelting by CW laser was performed by four consecutive scan passes under 45° with incremental rotation of 90° between passes. In addition to the parameters from Table 2, the focal plane was shifted towards the middle height of the inclined surface by moving the build cylinder up by $\Delta f = 2$ mm and $\Delta f = 1.3$ mm for powder removal and laser remelting, respectively.

The surface quality was assessed using a confocal focus variation microscope Sensofar S-Neox over an area of 8.7 x 4.2 mm and 4.7 x 4.7 mm for inclined and horizontal surfaces, respectively. Areal surface roughness Sa was calculated according to ISO 21920-2 filtered with a Gaussian filter with cut-off lengths λ_c=2.5 mm and λ_s=2.5 µm.

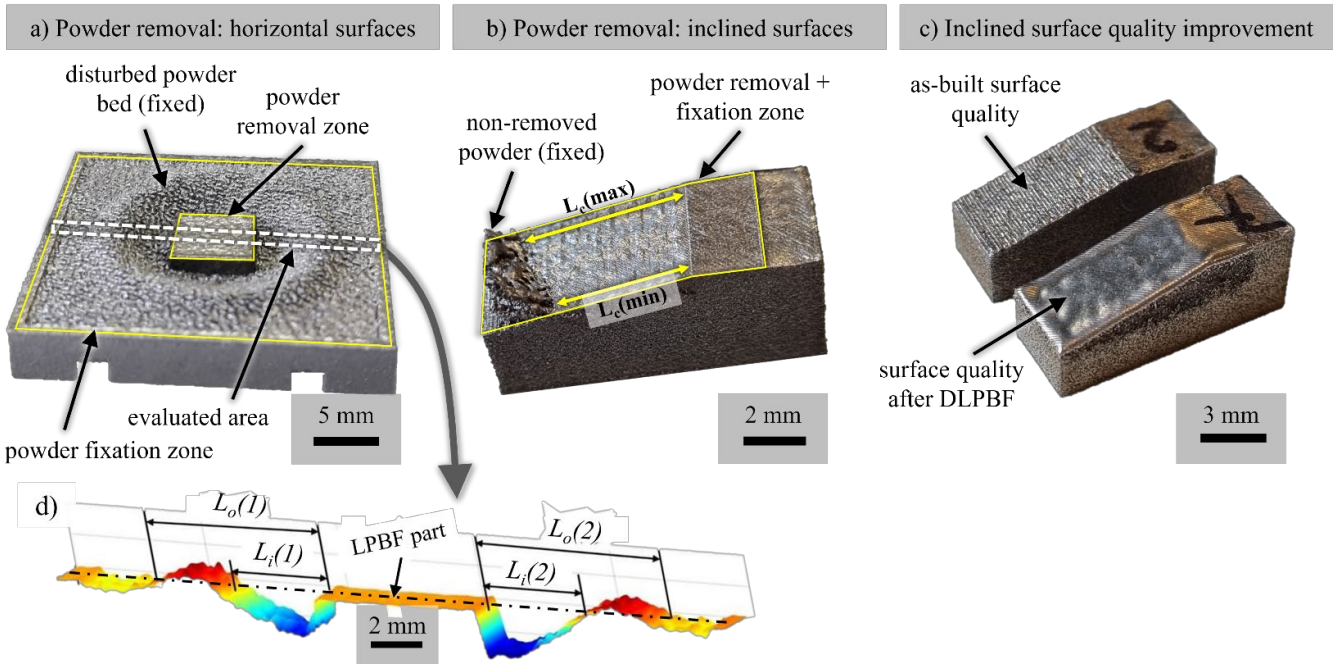

Figure 1: Methodology for (a) powder removal process study on horizontal surfaces, (b) powder removal applied to inclined surfaces, (c) combination of powder removal and laser remelting for surface quality improvement, (d) 3D measurement of the disturbed powder bed with L_i and L_o inner and outer disturbance length, respectively.

Table 1. Process parameters for powder removal using pulsed laser.

Material	M300/M789/A205/Ti64	M789
Sample geometry (surface orientation)	Cubic (horizontal)	Prism (15° inclined)
Average laser power, *P* [W]	25/30/35	42
Scanning speed, *v* [mm/s]	500/1000/1500	500
Hatch spacing, *h* [µm]	40	40
Pulse repetition rate , *PRR* [Hz]	100	100
Pulse duration, τ [ns]	10/20/30	30
Number of passes, *N*	1	1/3/5
Pulse to pulse distance *dp* [µm]	5/10/15	5
Pulse energy *Ep* [µJ]	250/300/350	420

Table 2. Process parameters for fixation of the powder bed and laser remelting using CW laser.

Process step	Powder fixation				Laser remelting
Material	M789	M300	A205	Ti64	M789
Sample geometry (surface orientation)	Cubic (horizontal)/ Prism (15° inclined)	Cubic (horizontal)			Prism (15° inclined)
Laser power, *P* [W]	100	100	100	100	200
Scanning speed, *v* [mm/s]	1500	1500	1500	1500	500
	1300	1300	1300	1300	
Hatch spacing, *h* [µm]	40	40	40	40	80
Number of passes, *N*	2	2	2	2	4

Results & Discussion

1. Powder removal using shock waves applied to various materials

In the first part of this study, the effect of the used material on the powder removal efficiency was investigated. Fig. 2 shows the main effects plot based on a L9 Taguchi design of experiments for the inner disturbance length L_i, which quantifies the disturbed powder bed around the parts. As shown in Fig. 2a-c, L_i exhibits similar trends for all investigated materials (M300, M789, A205, Ti64) within the selected parameter range. In agreement with the previously published results [8], the pulse duration τ has the most dominant impact on L_i, followed by pulse energy *Ep* and pulse-to-pulse distance *dp*. Further on, L_i and the generated shock wave efficiency appears to be higher with increasing pulse duration (Fig. 2c), pulse energy (Fig. 2b), and decreasing pulse-to-pulse distance (Fig. 2a). This becomes particularly evident for the pulse energy, as a larger amount of energy is deposited into the material, increasing the volume of interacting material. Consequently, a larger amount of material becomes available for vaporization and plasma formation, subsequently inducing the shock wave. The influence of the pulse-to-pulse distance on L_i might be partially explained by the number of pulses available for inducing shock waves. Considering a constant scanned length and area, as the pulse-to-pulse distance decreases, the number of pulses increases and so does the number of shock waves. This is in accordance with the point-strong-explosion theory [6], which describes pulses as the initiators of local explosions that cause shock waves.

The influence of pulse duration τ on L_i is less evident. Studies [14] have reported contrary findings to the present research, i.e. an increase in shock wave pressure with decreasing τ, as shorter τ lead to a higher peak power. However, a previous research on the used equipment [15] reported a non-linear dependence of the efficiency of the laser induced shock waves on τ (within the range 10-100 ns). This research confirmed a positive effect of increasing τ on the shock wave efficiency between 10-50 ns. This observation might be attributed to several phenomena associated with an extended laser-material interaction time and volume. Longer τ allow for interaction with a larger volume of material, potentially available for plasma formation and shock wave generation. This is supported by [8, 16] which reported a decrease of ablated material volume towards shorter τ in the same regime. Moreover, with an extended laser-material interaction time, the plasma plume has more time to form and expand before the exposure ends. This prolonged expansion could potentially enhance the strength of the shock wave, leading to an increased L_i. Nevertheless, as reported in [15], further increase in $\tau > 50$ ns resulted in a progressively reducing shock wave efficiency. As a matter of fact, the peak power decreases with increasing τ, consequently reducing the amount of evaporated material turned into plasma plume.

All investigated materials show similar trends, suggesting the occurrence of similar phenomena associated with the creation of laser-induced shock waves. However, there are variations in the magnitude of L_i. Compared to the tool steels (M789, M300), the mean L_i value for Ti64 is increased by 53.2 % and 32.5 %, respectively (Fig. 2d). The shock wave efficiency when processing A205 is comparable to Ti64, only 8.1 % lower. To understand the differences in mean L_i for the investigated materials, following aspects can be considered: (1) creation of shock waves, (2) displacement of the powder particles.

The creation of laser-induced shock waves is well-known for metals and relates to various material properties, including absorptivity, thermal conductivity, melting and vaporization temperature. In general, metals with higher absorptivity facilitate more efficient coupling of the pulse energy, and hence for heating. A low thermal conductivity promotes localized heating, which is beneficial for reaching the vaporization temperature. On the other hand, an increased thermal conductivity expands the heat-affected zone, increasing the volume of material potentially being available for material removal and thus the creation of shock waves.

A205 and Ti64 possess distinctively different material properties, yet both materials lead to a comparable shock wave efficiency. Ti64 exhibits a low thermal conductivity and high melting and vaporization temperature, on the other hand A205 has a high thermal conductivity and low melting and vaporization temperature. Hence, reaching the vaporization temperature in Ti64 should require a high pulse energy input. However, as the thermal conductivity is low, the metal is heated up rather locally and should be hence available for creating strong shock waves. In case of A205, reaching those threshold temperatures required less pulse energy, which possibly leads to an early onset of vaporization. As the melting and vaporization temperatures are comparably low, and the thermal conductivity high, it should promote an extended heat-affected zone with potentially an increased amount of material available for vaporization. On the other hand, compared to A205 and Ti64, the investigated steels have an intermediate level of thermal conductivity and melting and vaporization temperatures. Yet, the effect of shock waves on M300 and M789 is weaker compared to the lighter A205 and Ti64. Therefore, it cannot be

excluded that the generated shock waves are of a comparable magnitude for all the investigated materials. Hence, material density is another important factor to be considered. The low mass of the powder particles is expected to promote the disturbance of the powder bed, as they can be more easily displaced, which directly leads to an increase in L_i.

After investigating the effect of the used material on the shock wave efficiency, also the influence of extremely high roughness was studied. Such a roughness can be resulting from a high-productivity LPBF parameter set using a high layer thickness, such as reported in [13]. The L_i observed for highly rough M789 surfaces generated by LT 120 µm was not included in Fig. 2 as it appeared to be very small, hindering a proper detection with this methodology. Therefore, instead of studying the effect of the surface roughness on the powder removal efficiency applied to horizontal surfaces, the next section presents its application to inclined surfaces.

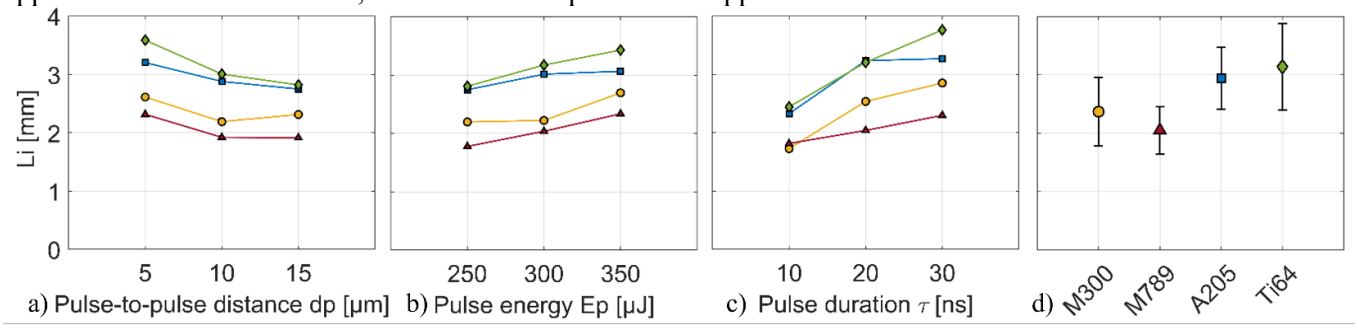

Figure 2: Main effects plot for inner powder bed disturbance L_i as a function of a) pulse-to-pulse distance, b) pulse energy, c) pulse duration, and d) mean inner disturbance length per material based on 9 samples each.

2. Powder removal efficiency on inclined surfaces

This section described the powder removal efficiency on 15° inclined surfaces from M789, produced with a standard (LT60) and a high layer thickness (LT120). Although using a high layer thickness can increase the LPBF process productivity up to 91% [13], LT120 surfaces exhibit significantly higher roughness compared to LT60. The roughness values for investigated samples are $Sa_{R,LT60}$=16.2 µm and $Sa_{R,LT120}$=24.0 µm, corresponding to an increase by 48.2%.

Fig. 3 shows the effect of number of scans (in powder removal) on the mean cleaned length L_c, serving as a measure of powder removal efficiency for parts with 15° inclined surfaces. L_c increases with the number of scan passes within the investigated range for both LT60 and LT120. Notably, LT60 exhibits a higher L_c for each investigated level of scan passes, up to 26.6% for N=1. However, the difference in powder removal efficiency for LT60 and LT120 appears lower with increasing scan passes, declining from 26.6% to 7.7% for N=1 and N=5 scan passes. Fig. 3 also shows that the difference between $L_c(max)$ and $L_c(min)$ reduces with increasing N for both LT60 and LT120. Although after N=1, a significant amount of powder is removed (high $L_c(max)$), low $L_c(min)$ values indicate only a small fully powder-free area. Fig. 4 visualizes an asymmetric ($L_c(max)>L_c(min)$) and an approximately rectangular cleaned area ($L_c(max)\approx L_c(min)$) for N=1 and N=5, respectively. A previous study [3] observed a similar phenomenon, attributing it to a redeposition of powder on the already cleaned surface. Due to the large powder volume covering the inclined surface during the first scan pass, the powder partially falls back on the already powder-free surface in the wake of the laser. With subsequent scan passes, the powder volume on the inclined surface decreases, and so does the redeposition of powder, resulting in an approximately rectangular cleaned area ($L_c(max)\approx L_c(min)$). Recent research has shown that powder can be entirely removed from inclined surfaces by further increasing the number of scan passes [3, 8, 9].

Powder removal via laser-induced shock-waves can be regarded as a surface phenomenon, given that both LT60 and LT120 were manufactured from the same powder material. As stated above, LT120 samples exhibit a significantly higher surface roughness. Consequently, the significant increased L_c for LT60 with N=1 scan pass can be attributed to the lower surface roughness. From the second powder removal pass, the process happens on a modified surface. The effect of powder removal on the surface was observed in [9], showing a significant increase of the overall surface texture for inclined surfaces after repeated powder removal. Fig. 3 shows that the amount of removed material per pass reduces with each following pass. Hence, this efficiency reduction could be attributed to the gradual deterioration of the initial high surface quality with each scan pass. The presence of large

roughness peaks and valleys could potentially dissipate energy, thereby reducing the available energy for shock wave generation. Additionally, the increased size of these surface features might dampen the propagation of shock waves and the motion of powder particles. A similar reasoning can be made for a decreased L_c on rough LT120 surfaces.

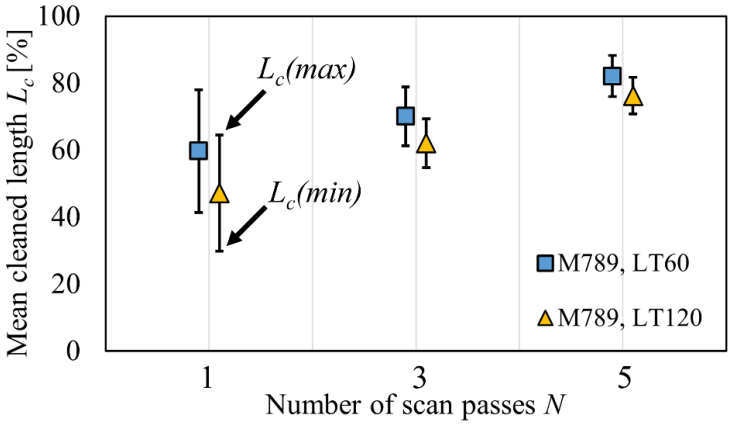

Figure 3: Mean cleaned length L_c given in % of absolute length of the inclined surface L_c(ref) as function of number of scan passes N, with the error bars indicating mean maximum and mean minimum cleaned length L_c(max), and L_c(min), respectively. Reported mean values are based on 6 samples each.

Figure 4: Top view on inclined surfaces of M789 samples after powder removal, a) LT60 surface after N=1, and LT120 surface after b) N=1 and c) N=5.

3. Proof of concept - Surface quality improvement

The proposed method has been successfully applied to improve the quality of inclined surfaces from M789, produced with a standard (LT60) and a high layer thickness (LT120). The powder covering the 15° inclined surface could be entirely removed via laser-induced shock waves, after N=15 and N=20 scan passes for LT60 and LT120, respectively. This is in agreement with the findings from above, showing an increased powder removal efficiency for LT60 surfaces. By remelting of the inclined surface the initial as-built surface roughness could be reduced from $Sa_{R,LT60}$=16.2 µm to 6.4 µm and $Sa_{R,LT120}$=24.0 µm to 16.4 µm for LT60 and LT120. This corresponds to a significant improvement by 61% and 32%, respectively. Surface quality improvement in this order of magnitude on inclined surfaces from M789 produced with LT60 has been previously reported [17]. Although laser remelting demonstrates a notable reduction in surface roughness for investigated surfaces, the effect of LT120 is more moderate. This can be attributed to the fact that laser remelting parameters were optimized for LT60 surfaces. Moreover the initial variation in surface roughness impacts the efficiency of laser remelting. Laser remelting involves redistributing of molten material from roughness peaks to valleys. As LT120 surfaces exhibit larger roughness peaks and valleys, the molten material needs to fill equally larger cavities.

Conclusion

This work demonstrates that the innovative Dual Laser Powder Bed Fusion strategy allows treating various AM metals during building (M300, M789, A205, Ti64), despite very different material properties. This technique combines selective powder removal via laser-induced shock waves and laser remelting during building. The powder removal efficiency on horizontal surfaces followed similar trends for all investigated materials (M300, M789, Ti64, A205), but the effect appeared to be stronger for lighter materials. It decreased with pulse-to-pulse distance, and increased with pulse energy and pulse duration. The pulse duration was found to have a dominant impact. The powder removal efficiency on inclined surfaces was examined on M789 parts inclined by 15°, produced with a standard (LT = 60 µm) and a high layer thickness (LT = 120 µm). The powder removal efficiency appeared to be higher on surfaces produced with LT60, which was attributed to the significantly lower surface roughness compared to LT120. However, the difference in powder removal efficiency for both LT appeared to decrease with the number of scan passes, suggesting a LT60 surface roughness deterioration due to the powder removal. Finally follows a demonstration of the quality improvement of 15° inclined surfaces from M789 parts by Dual Laser Powder Bed Fusion. After laser remelting a significant surface quality improvement was achieved, reducing Sa_R by 61% and 32% for LT60 and LT120, respectively.

The presented Dual Laser Powder Bed Fusion strategy allows treating various AM metals during building. The improvement of inclined surfaces manufactured with high layer thickness offers a significant value for additive manufacturing as it combines two typical contrary aspects: high productivity and improved surface quality. Moreover, as this treatment happens during building, it has the potential to reduce or eliminate the need of additional post-machining steps.

Acknowledgements

This research was funded by VLAIO/SIM/ICON HBC.2020.2958 MetaMould and by FWO/SB 1SB2322N. The authors would like to thank 3DSystems for providing certified building parameters for M789.

References

[1] J. Metelkova, L. Vanmunster, H. Haitjema, and B. Van Hooreweder, "Texture of inclined up-facing surfaces in laser powder bed fusion of metals," *Addit. Manuf.*, p. 101970, Mar. 2021, doi: 10.1016/j.addma.2021.101970.

[2] G. Strano, L. Hao, R. M. Everson, and K. E. Evans, "Surface roughness analysis, modelling and prediction in selective laser melting," *J. Mater. Process. Technol.*, vol. 213, no. 4, pp. 589–597, Apr. 2013, doi: 10.1016/j.jmatprotec.2012.11.011.

[3] J. Metelkova, D. Ordnung, Y. Kinds, and B. Van Hooreweder, "Novel strategy for quality improvement of up-facing inclined surfaces of LPBF parts by combining laser-induced shock waves and in situ laser remelting," *J. Mater. Process. Technol.*, vol. 290, p. 116981, Apr. 2021, doi: 10.1016/j.jmatprotec.2020.116981.

[4] S. S. Harilal, G. V. Miloshevsky, P. K. Diwakar, N. L. LaHaye, and A. Hassanein, "Experimental and computational study of complex shockwave dynamics in laser ablation plumes in argon atmosphere," *Phys. Plasmas*, vol. 19, no. 8, p. 083504, Aug. 2012, doi: 10.1063/1.4745867.

[5] B. Nagarajan, "Fabrication of 3D microfeatures on thin metal foils using laser-induced shock pressure," Ph.D. Thesis, Nanyang Technological University, Singapore, 2015.

[6] B. Campanella, S. Legnaioli, S. Pagnotta, F. Poggialini, and V. Palleschi, "Shock Waves in Laser-Induced Plasmas," *Atoms*, vol. 7, no. 2, Art. no. 2, Jun. 2019, doi: 10.3390/atoms7020057.

[7] C. Chung Ng, M. Savalani, and H. Chung Man, "Fabrication of magnesium using selective laser melting technique," *Rapid Prototyp. J.*, vol. 17, no. 6, pp. 479–490, Jan. 2011, doi: 10.1108/13552541111184206.

[8] J. Metelkova, D. Ordnung, Y. Kinds, A. Witvrouw, and B. Van Hooreweder, "Improving the quality of up-facing inclined surfaces in laser powder bed fusion of metals using a dual laser setup," *Procedia CIRP*, vol. 94, pp. 266–269, 2020, doi: 10.1016/j.procir.2020.09.050.

[9] J. Metelkova, L. Vanmunster, H. Haitjema, D. Ordnung, J.-P. Kruth, and B. Van Hooreweder, "Hybrid dual laser processing for improved quality of inclined up-facing surfaces in laser powder bed fusion of metals," *J. Mater. Process. Technol.*, vol. 298, p. 117263, Dec. 2021, doi: 10.1016/j.jmatprotec.2021.117263.

[10] C. Elangeswaran, K. Gurung, R. Koch, A. Cutolo, and B. Van Hooreweder, “Post-treatment selection for tailored fatigue performance of 18Ni300 maraging steel manufactured by laser powder bed fusion,” *Fatigue Fract. Eng. Mater. Struct.*, vol. 43, no. 10, pp. 2359–2375, 2020, doi: 10.1111/ffe.13304.
[11] A. Cutolo, C. Elangeswaran, G. K. Muralidharan, and B. Van Hooreweder, “On the role of building orientation and surface post-processes on the fatigue life of Ti-6Al-4V coupons manufactured by laser powder bed fusion,” *Mater. Sci. Eng. A*, vol. 840, p. 142747, Apr. 2022, doi: 10.1016/j.msea.2022.142747.
[12] E. Beevers, A. Cutolo, F. Mertens, and B. Van Hooreweder, “Unravelling the relation between Laser Powder Bed Fusion processing parameters and the mechanical behaviour of as built lattices in a novel Al–Cu–Mg–Ag–Ti–B alloy,” *J. Mater. Process. Technol.*, vol. 315, p. 117915, Jun. 2023, doi: 10.1016/j.jmatprotec.2023.117915.
[13] M. Sinico, J. Metelkova, T. Dalemans, L. Thijs, and B. Van Hooreweder, “High speed laser powder bed fusion of M789 tool steel with an optimized 120 µm layer thickness approach,” *Procedia CIRP*, vol. 111, pp. 162–165, Jan. 2022, doi: 10.1016/j.procir.2022.08.141.
[14] C. Oros, “Investigations involving shock waves generation and shock pressure measurement in direct ablation regime and confined ablation regime,” *Shock Waves*, vol. 11, no. 5, pp. 393–397, Apr. 2002, doi: 10.1007/s001930100112.
[15] J. Metelkova, “In-situ Laser Based Subtractive Manufacturing for Increased Precision of Metal Parts Produced by Laser Powder Bed Fusion.” PhD Thesis, KU Leuven, 2021.
[16] H. Herfurth, R. Patwa, T. Lauterborn, S. Heinemann, and H. Pantsar, “Micromachining with tailored nanosecond pulses,” in *Photonics North 2007*, SPIE, Oct. 2007, pp. 453–460. doi: 10.1117/12.778742.
[17] D. Ordnung, J. Metelkova, E. Vankersschaever, B. Van Hooreweder, “Investigation of an incremental dual Laser Powder Bed Fusion strategy for improving the quality of up-facing inclined surfaces,” *Procedia CIRP*, *111*, 101-104. 2022, doi: 10.1016/j.procir.2022.08.104